



HAL
open science

Curcumin derivatives: molecular basis of their anti-cancer activity

Valentina Basile, Erika Ferrari, Sandra Lazzari, Silvia Belluti, Francesca Pignedoli, Carol Imbriano

► To cite this version:

Valentina Basile, Erika Ferrari, Sandra Lazzari, Silvia Belluti, Francesca Pignedoli, et al.. Curcumin derivatives: molecular basis of their anti-cancer activity. *Biochemical Pharmacology*, 2009, 78 (10), pp.1305. 10.1016/j.bcp.2009.06.105 . hal-00522545

HAL Id: hal-00522545

<https://hal.science/hal-00522545>

Submitted on 1 Oct 2010

HAL is a multi-disciplinary open access archive for the deposit and dissemination of scientific research documents, whether they are published or not. The documents may come from teaching and research institutions in France or abroad, or from public or private research centers.

L'archive ouverte pluridisciplinaire **HAL**, est destinée au dépôt et à la diffusion de documents scientifiques de niveau recherche, publiés ou non, émanant des établissements d'enseignement et de recherche français ou étrangers, des laboratoires publics ou privés.

Accepted Manuscript

Title: Curcumin derivatives: molecular basis of their anti-cancer activity

Authors: Valentina Basile, Erika Ferrari, Sandra Lazzari, Silvia Belluti, Francesca Pignedoli, Carol Imbriano



PII: S0006-2952(09)00595-4
DOI: doi:10.1016/j.bcp.2009.06.105
Reference: BCP 10251

To appear in: *BCP*

Received date: 28-5-2009
Revised date: 24-6-2009
Accepted date: 26-6-2009

Please cite this article as: Basile V, Ferrari E, Lazzari S, Belluti S, Pignedoli F, Imbriano C, Curcumin derivatives: molecular basis of their anti-cancer activity, *Biochemical Pharmacology* (2008), doi:10.1016/j.bcp.2009.06.105

This is a PDF file of an unedited manuscript that has been accepted for publication. As a service to our customers we are providing this early version of the manuscript. The manuscript will undergo copyediting, typesetting, and review of the resulting proof before it is published in its final form. Please note that during the production process errors may be discovered which could affect the content, and all legal disclaimers that apply to the journal pertain.

Curcumin derivatives: molecular basis of their anti-cancer activity

Valentina Basile^a, Erika Ferrari^b, Sandra Lazzari^b, Silvia Belluti^a, Francesca Pignedoli^b and Carol Imbriano^{a*}.

^aDipartimento di Biologia Animale, Università di Modena e Reggio Emilia, via Campi 213/D, Modena; ^bDipartimento di Chimica, Università di Modena e Reggio Emilia, via Campi 183, Modena.

*Corresponding author. Tel: +39-059-2055542; Fax: +39-059-2055548. E-mail address: cimbriano@unimo.it; carol.imbriano@unimore.it

Abbreviations: bDMC, *bis*-DemethoxyCurcumin; DAC, diAcetylCurcumin; MIT, microtubule-targeting agents; BrdU, bromodeoxyuridine; PI, propidium iodide; DMSO, dimethylsulfoxide; DSB, double strand break; FACS, Fluorescence Activated Cell Sorter, ChIP, Chromatin immunoprecipitation; ATM, Ataxia Telangiectasia Mutated; ATR, ATM and Rad3-related.

Abstract

Curcumin, a phenolic compound from the plant *Curcuma longa L.*, has shown a wide-spectrum of chemopreventive, anti-oxidant and anti-tumor properties. Although its promising chemotherapeutic activity, preclinical and clinical studies highlight Curcumin limited therapeutic application due to its instability in physiological conditions. To improve its stability and activity, many derivatives have been synthesized and studied, among which *bis*-DemethoxyCurcumin (bDMC) and diAcetylCurcumin (DAC). In this report, we show that both bDMC and DAC are more stable than Curcumin in physiological medium. To explore the mechanism of their chemotherapeutic effect, we studied their role in proliferation in the HCT116 human colon cancer cells. We correlated kinetic stability and cellular uptake data to their biological effects. Both bDMC and DAC impair correct spindles formation and induce a p53- and p21^{CIP1/WAF1}- independent mitotic arrest, which is more stable and long-lasting for bDMC. A subsequent p53/p21^{CIP1/WAF1}- dependent inhibition of G1 to S transition is triggered by Curcumin and DAC as a consequence of the mitotic slippage, preventing postmitotic cells from re-entering the cell cycle. Conversely, the G1/S arrest induced by bDMC is a direct effect of the drug and concomitant to the mitotic block. Finally, we demonstrate that bDMC induces rapid DNA double-strand breaks, moving for its possible development in anti-cancer clinical applications.

Keywords: Natural compounds; Curcumin analogs; cell cycle regulation; p53; DNA damaging agents.

1. Introduction

The rapid dynamics of spindle microtubules are essential to proper spindle function. Microtubules are favorite target of naturally occurring toxic molecules, most of which are produced by a large number of plants (reviewed in [1]). In fact, many microtubule-targeting agents (MTAs) have been discovered by screening natural products and are currently in clinical trials. Curcumin, a common flavoring agent in the spice turmeric, perturbs microtubule assembly dynamics through tubulin binding, which results in its conformational changes [2]. Significant depolymerization of interphase microtubules and mitotic spindle microtubules have been observed after Curcumin incubation of HeLa, MCF-7, HT-29 and HCT-15 cells, thus leading to a mitotic arrest [2-4].

Curcumin exhibits cancer growth inhibition both *in vitro* and *in vivo* [5, 6]: it suppresses cell proliferation in a variety of cancer cell lines and it inhibits tumorigenesis [7-17]. Multiple mechanisms of action are likely responsible for Curcumin various effects on cancer cells: G1/S arrest and apoptosis induction have been observed other than the mitotic block in different tumor cell lines [18-20]. Experimental evidence reveals a multitude of molecular targets, including transcription factors, cell cycle proteins, enzymes, cell surface adhesion protein and cytokines [21, 22].

Although Curcumin has an evident anti-cancer activity, relative poor stability has been highlighted as one of the major problems in therapeutic applications. Stability in cell culture medium containing 10% FBS or in human blood is greater than in phosphate buffer, but 50% of the molecule has still decomposed after 8 hours [23, 24].

To enhance metabolic stability and antiproliferative activity against human cancer cells, various Curcumin analogs have been synthesized, among which *bis*-DemethoxyCurcumin (bDMC) and diAcetylCurcumin (DAC) (Fig.1) (reviewed in [25]). Although bDMC differs from its lead-compound in the chemical structure only with regard to methoxy substitution, it exhibits significantly different antioxidant, antitumor, and anti-inflammatory activities. bDMC shows higher cytotoxicity against human ovarian cancer cell line, increased antimutagenic, anticarcinogenic and antioxidant activity (reviewed in [25]). The inhibition of cancer cell invasion by bDMC highlights its enhanced

antimetastasis potency [26]. The synthetic derivative DAC shows higher antibacterial activity against multiresistant bacteria [27] and a stronger nitric oxide (NO) and O_2^- anion scavenging activity [28, 29], although it has slightly lower apoptotic activity on AK-5 rat histiocytoma cells [30]. Whether bDMC and DAC analogues have the same Curcumin molecular targets is also not clear at present.

The aim of our study is to shed light on the potential anti-cancer effects of bDMC and DAC against human colon cancer cells, unraveling the molecular basis of their biological activity. Understanding molecular events that lead these molecules to arrest cell proliferation is an important prerequisite for their development as chemotherapeutic agents. We show here that both bDMC and DAC have increased stability in physiological medium and improved nuclear cellular uptake compared to Curcumin. Cellular and molecular analyses of the effects of bDMC and DAC in HCT116 cells have been performed to define their activity in cell cycle modulation. We demonstrate that bDMC causes a concomitant G1/S and mitotic block, triggering rapid DNA double-strand breaks. Finally, we investigate the role of the two main inhibitors of the cell cycle, p53 and p21^{CIP1/WAF1}, in mediating the cell cycle impairment induced by bDMC and DAC.

2. Materials and methods

2.1 General Procedures. Spectrophotometric measurements were performed using Jasco V-570 spectrophotometer at $25 \pm 0.1^\circ\text{C}$ in the 200-600 nm spectral range employing 1 mm quartz cells. NMR Spectra were recorded on a Bruker Avance AMX-400 spectrometer with a Broad Band 5mm probe (inverse detection). Nominal frequencies are 100.13 MHz for ^{13}C and 400.13 MHz for ^1H . The typical acquisition parameters for ^1H were as follows: 20 ppm spectral bandwidth (SW), 6.1 μs pulse width (90° pulse hard pulse on ^1H), 0.5-1s pulse delay, 216-512 number of scans. For 2D H,H-Homonuclear Correlated Spettroscopy (COSY) typical parameters were used. For 2D H,X-Hetero Correlated Spettroscopy, HMBC and HMQC oportune parameters were used ($50\text{-}90^\circ$ pulses; 32k data points; 1 s relaxation delay; 8-64k transients; $^1J_{\text{H-C}}$ 125-145 Hz; $^3J_{\text{H-C}}$ 5-15 Hz). Methanol- d_4 (CD_3OD) and DMSO- d_6 (DMSO) were used as NMR solvent. All reported chemical shifts are referred to TMS.

2.2 Preparation of Curcuminoids. A suspension of B_2O_3 (1 mmol) and acetylacetone (1 mmol) in DMF (1.5 ml) was stirred for 30 minutes at 80°C , then tributylborate (4 mmol) was added. After 30 minutes, the appropriate benzaldehyde (1.8 mmol) was added and followed by slow addition of *n*-butylamine (0.4 mmol in 0.5 ml of DMF). After stirring at 80°C for 4 hours, the solution was acidified with 0.5 M HCl (8 ml) and cooled down to room temperature. The yellow-orange solid was re-suspended in water, filtered and dried *under vacuum*. Purity of all synthesized compounds was $>98\%$, and it was determined by means of NMR techniques and combustion analysis.

Curcumin -1,7-bis[3-methoxy-4-hydroxyphenyl]hepta-1,6-diene-3,5-dione

^1H NMR (CD_3OD): δ 5.95 (s, 1H; H-1), 6.61 (d, $J=15.8$ Hz, 2H; H-3), 7.56 (d, $J=15.8$ Hz, 2H; H-4), 7.20 (d, $J=2$ Hz, 2H; H-6), 6.82 (dd, $J=8.0$, 1Hz, 2H; H-9), 7.09 (dd, $J=8.0$, 2 Hz, 2H; H-10). ^{13}C NMR (CD_3OD): δ 100.2 (C-1), 183.7 (C-2), 120.6 (C-3), 140.4 (C-4), 127.3 (C-5), 110.1 (C-6), 147.8 (C-7), 149.0 (C-8), 115.0 (C-9), 122.6 (C-10). Anal. Calc. (found) for $\text{C}_{21}\text{H}_{20}\text{O}_6$: C 68.47 (68.41), H 5.47 (5.52); yield 60%. m.p. 180°C .

DiacetylCurcumin (DAC) - 1,7-bis[3-methoxy-4-acetylphenyl]hepta-1,6-diene-3,5-dione

^1H NMR (CD_3OD): δ 5.94 (s, 1H; H-1), 6.59 (d, $J=15.9$ Hz, 2H; H-3), 7.57(d, $J=15.9$ Hz, 2H; H-4), 7.49 (d, $J=2$ Hz, 2H; H-6), 6.82 (dd, $J=7.5$, 1Hz, 2H; H-9), 7.49 (dd, $J=7.5$, 2 Hz, 2H; H-10). ^{13}C NMR (CD_3OD): δ 100.3 (C-1), 183.6 (C-2), 120.4 (C-3), 140.2 (C-4), 126.5 (C-5), 129.3 (C-6), 115.3 (C-7), 160.1 (C-8), 115.3 (C-9), 129.3 (C-10). Anal. Calc. (Found) for $\text{C}_{25}\text{H}_{24}\text{O}_8$: C 66.36 (65.91), H 5.35 (5.73); yield 87%. m.p. 171 °C.

BisDemethoxyCurcumin (bDMC) - 1,7-bis[4-hydroxyphenyl]hepta-1,6-diene-3,5-dione

^1H NMR ($\text{DMSO}-d_6$): δ 6.13 (s, 1H; H-1), H-3 6.79, H-4 7.63, H-6 7.66, H-7 6.92, H-9 6.92, H-10 7.66; C-1 100.8, C-2 183.4, C-3 120.8, C-4 140.3, C-5 125.8, C-6 130.2, C-7 115.9, C-8 159.8, C-9 115.9, C-10 130.2. Anal. Calc. (Found) for $\text{C}_{19}\text{H}_{16}\text{O}_4$: C 74.01 (73.95), H 5.23 (5.31), yield 75%. m.p. 217°C.

2.3 Cell lines and drugs. HCT116, derived from a human colorectal carcinoma, HCT116/E6 and HCT116 p21 $-/-$ were generously provided by Bert Vogelstein (Johns Hopkins University School of Medicine, Baltimore, MD). The HCT116 and HCT116 p21 $-/-$ cell lines were cultured in IMDM medium supplemented with 10% FCS. HCT116/E6 were grown with G418 (500 ng/ml). Drugs were added to cell medium at the concentration described in the text for 4, 8, 16 or 24 hours. IC_{50} concentrations after 24 hours treatments were estimated in 10 μM and 30 μM for Curcumin/DAC and bDMC respectively. Cells were treated with Nocodazole (0,5 μM) for 16 hours and with Adriamycin (1.3 μM) for 24 hours.

2.4 Uptake measurements. Culture medium (3 ml) was acidified with 6N HCl (1:1 (v/v)) and vortexed for 30 s. Following addition of 3 ml of extracting buffer (ethyl acetate and isopropanol 9:1 (v/v)), samples were vortexed and shaken in the Orbital shaker (at 100 rpm) for 15 min. After centrifugation at 18000 rpm for 20 min, the upper organic layer was filtered through a membrane filter (0.22 μm) and directed to UV-vis analysis.

The cell pellets were resuspended in RIPA buffer (20 mM Tris/HCl at pH 8.0, 137 mM NaCl, 10 % of glycerol, 5 mM EDTA, 1 mM phenylmethyl-sulfonyl fluoride and protease inhibitor cocktail) and the cell-liquid extraction was carried out. The cell extracts were cleared by centrifugation at 18000

rpm for 15 min and acidified by 6N HCl (1:1 v/v) and vortexed for 30 s. Then the same extracting procedure as for culture medium was performed.

2.5 Flow cytometric cell cycle analysis. 500 000 cells were harvested after drug treatments and DNA distribution analysis of PI and BrdU stained cells was performed by an Epics cytofluorimeter (Beckman Coulter) [31, 32]. Anti-BrdU antibody was provided by BioLegend (#317902) and mouse anti-FITC by Dako (#F0313).

2.6 Cellular extracts and immunoblotting. Total extracts were prepared by resuspending the cell pellet (300 000 cells) in 200 μ l of lysis buffer (50m mM Tris-HCl pH 8.0, 120 mM NaCl, 0.5% NP-40, 1 mM EDTA, protease and phosphatase inhibitors). Immunoblot analysis of histones was performed using HCT116 acid extracts. Briefly, the cell pellet was suspended in lysis buffer (10 mM HEPES pH 7.9, 1.5 mM MgCl₂, 10 mM KCl), added of hydrochloric acid 0.2 N, incubated on ice for 30 minutes and cleared by high-speed centrifugation for 10 minutes at 4°C.

For immunoblotting equivalent amounts of total extracts (50 μ g) were resolved by SDS-PAGE, electrotransferred to nitrocellulose membrane, and immunoblotted with the following primary antibodies diluted 1:1000 in TBS 1X/BSA 1mg/ml: anti-CycB1 (Active Motif #39504), anti-p53 DO-1 (Santa Cruz #sc-126), anti-phospho-H2AX (Cell-Signaling #2577), anti-H2A acid-patch (Active Motif), anti-phosphoATM Ser1981 (Cell-Signaling #4526), anti-p21 (Upstate) and anti-actin (Santa-Cruz).

2.7 Immunofluorescence. 300 000 cells were seeded on coverslips the day before treatments. After drugs incubation, cells were washed twice in PBS 1X at room temperature, fixed in cold methanol/acetone for 2 minutes and permeabilized with 0.05% TritonX 100 in PBS 1X for 5 minutes. Samples were preincubated with PBS 1X/BSA 1% for 15 minutes and then incubated overnight at 4°C with the following primary antibodies diluted 1:100 in PBS 1X/BSA 1%: anti-phospho-Histone H2AX (Ser139) (Upstate #05-636; Active Motif #39117) and anti-tubulin (Sigma-Aldrich). Cells were then washed twice with PBS 1X and incubated 15 minutes at room temperature in PBS 1X/BSA 1% before a further incubation for 60 minutes at room temperature in the dark, with Hoechst and the relative secondary antibodies sheep anti-rabbit FITC-conjugate

1:200 (Sigma, F7512) and goat anti-mouse TRITC-conjugate 1:150 (Sigma, T5393). After three washes with PBS 1X monolayers were mounted with Vectashield and examined with Zeiss AxioSkop 40 fluorescence microscope (Carl Zeiss, Jena, Germany), images collected with a AxioCam HRc camera and AxioVision version 3.1 software package. The same samples were analyzed by confocal microscopy (Leica DM IRE2).

2.8 RT-PCR analysis. RNA was extracted from cells untreated or treated with the described drugs by using RNeasy kit (Qiagen, Hilden, Germany), according to the manufacturer's protocol. For cDNA synthesis, 5 μ g of RNA were retrotranscribed with a Moloney murine leukemia virus reverse transcriptase (RT) (Promega). Semiquantitative PCRs were performed with oligonucleotides previously described [31, 32].

2.9 Chromatin immunoprecipitation assay. Chromatin immunoprecipitations were essentially performed as described previously [31, 32]. Chromatin was prepared upon 24h drugs treatment and immunoprecipitated with anti-p53 (DO-1, Santa-Cruz) and anti-Flag (Sigma-Aldrich) antibodies. PCRs were performed with the following oligonucleotides:

p21_for:GTAAATCCTTGCCTGCCAGAGTG; p21_rev: GCTGCCAGCGCCGAGCCAG

2.10 Statistical analysis. Results are shown as means \pm SD. Statistical analysis for the results of western blot of Fig. 4B was done using one-way ANOVA, followed by Bonferroni's *t*-test to determine whether there were differences between specific groups (DMSO vs each curcuminoid).

3 Results

3.1 Uptake of Curcumin and its derivatives in HCT116 cells.

Although Curcumin has been extensively investigated as it concerns its anti-cancer activity in a variety of cell types, only few studies provide uptake data [33, 34] and none correlates kinetic stability of natural and synthetic Curcuminoids to their cellular uptake. A preliminary kinetic study was performed for bDMC and DAC (Fig. 1), in order to evaluate their stability in culture medium compared to Curcumin. A representative fluorescence spectrum of Curcumin maintained in culture medium for 4 and 24 hours is given in Figure 2A (left panel). Absorbance of Curcumin dramatically decreased in the first 4 hours (~ 50%), and then smoothly diminished up to 24 hours (~ 10%), suggesting a *pseudo*-first order kinetic process (Fig. 2A, right panel). Differently, bDMC and DAC maintained almost the same absorbance values in the first 24 hours, hinting their greater stability with respect to Curcumin.

Cellular uptake and intracellular localization of the drugs were evaluated by confocal microscopy analysis of HCT116 cells treated with the estimated IC_{50} concentrations for 24 hours. All the molecules showed mainly a cytoplasmic fluorescence, although nuclear staining appeared to be more intense in cells treated with bDMC and DAC than Curcumin (Fig. 2B, arrows).

The kinetic of cellular uptake was determined by UV-vis analysis. Figure 2C shows the histogram of the percentages of Curcumin, bDMC and DAC (20 μ M and 30 μ M) extracted from HCT116 cells and their relative culture media as a function of time incubation; all data have been normalized taking into account the absorbance decreases observed after 4 and 24 hours due to the relative stability of each drug (Fig. 2A). The percentages determined both inside the cell and in culture medium were almost independent of drugs concentration. During 4 hours-treatment, the drug percentage in culture medium was around an averaged value of 70% for all Curcuminoids, even if data (30 μ M) suggested the following order of uptake: bDMC > DAC > Curcumin. Although the sum of cell and culture medium percentages should represent 100%, after 4 hours-treatment only Curcumin followed this prediction. For both bDMC and DAC the sum of the two percentages was 75% and 80% respectively, hinting that the missing quantity should have followed different

metabolic and/or degradation processes inside the cell. The strong decrease in culture medium percentage observed for Curcumin and bDMC after 24h treatment suggested their incremented uptake. No changes in drug distribution were observed comparing 4 and 24 hours incubations with DAC, indicating that longer time exposition didn't increase its cell absorption.

Figure 2D reports the absolute percentages referred to time zero concentration inside the cell for each drug (20 μ M and 30 μ M) at 4 and 24 hours. A dose-dependent uptake was observed for Curcumin and bDMC (same percentage independently on drug treatment concentration), while for DAC an increased value was detected as concentration was risen up. After 24 hours the amount of Curcumin and bDMC inside the cell was respectively < 2% and < 0.5 %, while DAC showed higher percentages (>3% for 20 μ M and >7% for 30 μ M).

These data indicate that, although DAC and bDMC have similar stability in culture medium, they follow different metabolism inside the cell: DAC exhibited a limited decomposition up to 24 hours while bDMC was fastly uptaken and metabolized already during the first 4 hours of treatment.

3.2 Treatment of HCT116 cells with Curcumin derivatives delays mitotic exit.

The effects of Curcumin on cell cycle arrest are associated with structural changes of tubulin, followed by abnormal chromosome segregation [2, 3]. To determine whether bDMC and DAC exert an effect on mitotic spindle organization, HCT116 cells treated for 24 hours with IC₅₀ doses were fixed and processed for immunofluorescence microscopy using anti-tubulin antibody and HOECHST to detect nuclear morphology. Compared with DMSO treated cells, incubation with Curcumin, bDMC and DAC resulted in aberrant mitotic figures with monopolar microtubule spindles, indicative of alterations on microtubule polymerization (Fig. 3A, arrows).

Microtubule spindle impairment generally hampers the chromosome alignment, thus blocking cells in mitosis, specifically at the onset of the anaphase, until spindle formation is completed [1, 35]. To assess whether the observed monopolar spindles led to any effect on cell cycle progression, we evaluated the distribution of the cells throughout the cell cycle by PI/FACS analysis.

We determined the IC₅₀ values and a preliminary dose-response experiment was run with each curcuminoid for 24 hours (Suppl. Fig.1). We decided to perform our next experiments treating cells with IC₅₀ estimated concentrations (Curcumin 10 μM, bDMC 30 μM and DAC 10 μM).

The average of ten independent experiments indicated that 24 hours-treatment induced a more evident G2/M arrest for Curcumin (63%) and DAC (62%) compared to bDMC (51%) (Fig. 3B). Unlike the well known microtubule active drug nocodazole, G1 cells were not completely lost but a clear decrease was observed with respect to control/DMSO. DNA replication was investigated by BrdU/PI FACScan analysis: a robust decrease was observed for Curcumin (11%), bDMC (16%) and DAC (10%) relative to DMSO treated cells (40%), associated to a G2/M arrest (from 20% in DMSO to about 57% in Curcumin and DAC and only 49% in bDMC treated cells) (Fig. 3C). No polyploid cells (DNA content > 4C) were detected after 24 hours treatments in HCT116 cells. The analysis of equal amounts of cell lysates by western blot highlighted an increase of phosphorylated histone H3 at serine 10 (H3Ser10), which has been recognized as cell cycle marker to evaluate the late-G2/M status of cells. The comparison between H3Ser10 *versus* total H2A protein expression was consistent with the lower percentage of mitotic cells after bDMC treatment (Fig. 3D).

3.3 Bis-DemethoxyCurcumin triggers a concurrent G1/S and mitotic arrest.

Prolonged mitotic arrest can lead cells (i) to apoptosis or (ii) to escape mitosis *via* mitotic slippage through the ubiquitination and proteolysis of Cyclin B [36]. Mitotic slippage leads to the accumulation of postmitotic G1 cells, which are subsequently arrested in their cell cycle progression by activating a p53-dependent G1 checkpoint [37, 38, 39].

To determine whether G1 cells resulted from escaped progression through mitosis and cytokinesis rather than a direct G1 arrest, we pulsed HCT116 with BrdU for 1 hour before drug treatments (Fig. 4A). After Curcumin and DAC incubation about 45% of the total G1 cells was found to be BrdU labeled, hinting that about one-half of G1 cells were originated by cells that failed to arrest in G2/M. Conversely, by treating cells with bDMC, G1 cells were almost found to be BrdU unlabeled (77%), suggesting that this population has originated from cells that were already in G1 before the incubation with BrdU. These data pointed out a more stable mitotic block after bDMC with respect

to Curcumin and DAC (only the 23% of BrdU labeled cells escaped from the G2/M block compared to 55-60% after Curcumin and DAC incubation). To further confirm that Curcumin and DAC treated cells exit mitosis *via* mitotic slippage, we evaluated Cyclin B1 expression levels. Western blot analysis demonstrated that Cyclin B1 levels decreased upon Curcumin, bDMC and DAC incubation compared to DMSO (Fig. 4B, upper panel). Differently from bDMC treated cells, in which protein reduction was associated to its transcriptional inhibition, the decreased Cyclin B1 staining after Curcumin and DAC exposure could be ascribed to its proteolysis, as RT-PCR analysis didn't show changes in gene transcription (Fig. 4B, lower panel).

We next determined whether bDMC could induce a long lasting block in cell cycle progression by drug-release experiments. The release from the mitotic block induced by bDMC was slowed down up to 12 hours and was associated to a modest increase in G0/G1 events compared to Curcumin and DAC (Fig. 4C).

To characterize the G1/S arrest induced by bDMC, we performed synchronization–release experiments and we analyzed S-phase entry. The experimental design is outlined schematically in Figure 4D. Serum depletion for 24 h (0.5% FCS) resulted in G0/G1 arrest of HCT116 (between 80 and 85%); S phase fractions were determined by quantifying BrdU incorporation after release into 10% FCS fresh media added with each drug. Upon 10 up to 14 hours from the release in DMSO, Curcumin and DAC, about 18%-30% of cells clearly shifted to early S phase. A delay from S to G2/M was then observed for Curcumin and DAC compared to control cells: DMSO-release shifted about 35% of cells to G2/M after 18 hours, while the same percentage was reached after 22 hours with Curcumin (31%) and DAC (30%), explaining the lack of the G2/M block usually observed after 24 hours-treatment. With regards to bDMC, the kinetic of the release from G0/G1 to early S was comparable to Curcumin and DAC; conversely, BrdU positive cells were clearly inhibited from early to late S. After 22 hours, about 60% of cells were still retained in synthesis. The release in nocodazole-medium demonstrated that cells took 14 hours to accumulate in synthesis (36%), similarly to DMSO (35%), and after 22 hours were completely shifted in G2/M (96.9%).

3.4 Bis-DemethoxyCurcumin induces DNA damage concomitantly to the cell cycle block.

Many human cells exposed to MITs acquire DNA damage causing a significant delay in mitotic exit upon removal of the block [40, 41].

Compared to Curcumin and DAC, bDMC showed a slower kinetic in re-entering the cell cycle after the release, hinting the possibility that it might induce DNA damage during the cell cycle block.

To explore this possibility, we examined by western blot the activation of γ -H2AX, which is known to be phosphorylated rapidly at Ser 139 in response to DNA DSBs. All the Curcuminoids induced γ -H2AX after 24 hours-treatment (Fig. 5A). The normalization with respect to the total amount of H2A indicated that the strongest H2AX phosphorylation was triggered by bDMC, similarly to the effects of Adriamycin, a potent antitumor drug that induces DNA DSBs.

To investigate the possible interaction between the cell cycle impairment and DNA damage we performed a time course experiment. PI cell cycle analysis and γ -H2AX immunofluorescence were carried out on 8, 16 and 24 hours-treated cells. 16 hours incubation accumulated cells in G2/M as efficiently as 24 hours (Fig. 5B, right panel). Interestingly, only bDMC induced γ -H2AX already upon 16 hours treatment (Fig. 5B, left panel). These data suggest that bDMC-induced DNA damage is concurrent to the cell cycle arrest, while DSBs observed after Curcumin and DAC incubation can be the effect of a prolonged mitotic block.

DSBs are most closely associated to H2AX phosphorylation by ATM activation, which acts as a regulator of cell cycle checkpoint and DNA repair [42]. The ATM/ATR- dependent pathway triggers cell cycle arrest until DNA integrity is restored by repair processes [43, 44]. ATM activation after Curcuminoids treatment was explored by the analysis of Ser1981 phosphorylation. Phospho-ATM was detected after Curcumin, bDMC and DAC incubation, but not after DMSO addition (Fig. 5C). Co-incubation of cells with a non toxic dose of caffeine (1mM), which inhibits ATM/ATR, didn't result in the release of cells from the G2/M arrest, suggesting that ATM activation didn't participate in maintaining the mitotic block induced by Curcuminoids (Fig. 5D).

3.5 Inactivation of p53 and p21 abrogates the post-mitotic G1 arrest.

As cellular insults (*e.g.* DNA damage and microtubule disruption) induce signaling pathways which mediate p53 activation, we investigated p53 expression levels after Curcuminoids treatment.

Western blot shown in Figure 5C clearly detected an increase of p53, particularly after bDMC exposure.

Which is the role of p53 in cell cycle arrest induced by Curcumin and its derivatives has not been yet elucidated. We therefore analyzed cell cycle progression in HCT116/E6 cells, in which p53 is inhibited by the overexpression of the viral protein E6. Cell cycle phase distributions showed that p53 didn't participate to the G2/M block induced by Curcumin, bDMC and DAC (Fig. 6A). The comparison between HCT116 (Fig. 3B) and HCT116/E6 (Fig. 6A) clearly highlighted that p53 inhibition even induces a more robust G2/M arrest. Compared to HCT116, G0/G1 cells were reduced of about 50%, while S cells increased of about 50-60% upon Curcumin and DAC treatments. No effect on DNA replication (S phase) was even observed after bDMC incubation compared to DMSO. Nocodazole treatment of HCT116/E6 didn't show any difference in cell cycle phase distribution compared to HCT116. These data suggest that one of the main determinant in the subsequent fate after prolonged mitotic arrest is whether the cells can functionally activate p53 and its pathway. Cells entering mitosis in the presence of microtubule drugs can escape mitosis and subsequently arrest in the next G1 by p53 activation. Differently, cells lacking p53 survive and reproduce, as suggested by the increase of S phase. The role of p53 in controlling G1 to S passage is more evident for bDMC, as the G1/S block is a direct effect of the drug.

The CDK-inhibitor p21^{CIP1/WAF1} is induced after DNA damage and plays a role in the G1 arrest, but not in preventing G2 progression [37]. p21 was overexpressed after Curcuminoids treatment compared to control cells (Fig. 6B, upper panel). Nocodazole treatment, which accumulated a higher percentage of mitotic cells, didn't show higher p21 levels, suggesting that its activation is not triggered by the inability to exit mitosis. p21 transcriptional activation has been shown to be both p53-dependent and -independent. To elucidate the role of p53 in mediating p21 overexpression we performed RT-PCR and western blot analysis in HCT116 cells compared to HCT116/E6 cells. Figure 6B (lower panel) shows that p21 was activated also in the absence of p53, and a higher expression was still detected upon bDMC treatment. There is evidence suggesting that Curcumin antiproliferative effect is mediated by p21-induced cell cycle arrest, even if it has been recently

demonstrated that in HCT116 cells Curcumin induces apoptosis in a p21-independent manner [45]. To understand whether p21 was necessary to inhibit cell cycle progression after Curcuminoids treatments, we performed PI cell cycle analysis of HCT116 p21^{-/-} treated cells (Fig. 6C). With respect to HCT116/E6 cells, a further decrease of G0/G1 and an increase of G2/M events were detected, while no differences in S phase were observed following Curcumin and DAC incubation. bDMC showed even an increase of replicative events with respect to DMSO (28% *versus* 19%). To elucidate whether transcriptional activation of p21 was mediated by p53, we performed a CHIP analysis with chromatin from HCT116 treated cells immunoprecipitated with anti-p53 and anti-Flag as unrelated antibody. Figure 6D shows that after Curcumin and DAC treatment p53 was recruited to the p21 promoter. On the other hand, only a weak binding of p53 was observed upon bDMC incubation, thus suggesting that bDMC induces a p53-independent activation of the p21 gene. Thus, we concluded that both p53 and p21 are not involved in mediating the G2 arrest induced by Curcuminoids, but they are likely required to maintain G1 arrested cells, which originate as a consequence of mitotic slippage for Curcumin and DAC, rather than a direct G1/S block for bDMC.

4. Discussion

Although phase I clinical trials demonstrated that Curcumin is well-tolerated orally and no dose-limiting toxicity was observed [5, 46], it has poor bioavailability and may undergo intestinal metabolism, which can be to a great extent the consequence of its deficient pharmaceutical profile [21, 47, 48]. Currently, Curcumin derivatives represent a well-established strategy to enhance metabolic stability and therefore anti-proliferative activity against human cancer cells. In this report, we have investigated the analogs bDMC and DAC through biochemical and molecular studies with the aim to identify the connections between structure and mode of action.

It has been recently demonstrated that the deletion of β -diketone moiety enhances *in vitro* the stability of Curcumin in pH 7.4 condition [49]. We show that bDMC and DAC, although preserving the β -diketone, are more stable than Curcumin in culture medium, hinting that the degradation mechanisms of Curcuminoids are probably connected to the presence of a strong *intra*-molecular hydrogen bond between the vicinal hydroxy and methoxy groups. DAC exhibits a limited decomposition both in culture medium and inside the cell. Differently, increased stability of bDMC in culture medium is coupled with lower cellular concentration, suggesting that it is easily metabolized or conjugated to other molecules into the cells, leading to a quick biological response (Fig. 1).

Even if both DAC and bDMC show the same effect on microtubule spindle organization (Fig. 3A), the analysis of cell cycle progression in HCT116 cells corroborates the hypothesis that the two analogs may have different properties and activities. While DAC treatment induces a delayed mitotic exit comparable to Curcumin, bDMC exposure results in a concomitant mitotic and G1/S block. Additionally, the BrdU pulse/chase experiment (Fig. 4A) indicates that, although less robust, the mitotic arrest induced by bDMC is more stable with respect to Curcumin and DAC. A higher percentage of BrdU labeled G1 cells can be detected upon Curcumin and DAC prolonged treatments compared to bDMC, hinting that cells exiting mitosis subsequently accumulate in G1 and are prevented from S phase entry. bDMC long-lasting block is further supported by drug-release experiments.

We demonstrate that p53 is not required for the mitotic arrest induced by microtubule poisons, but the experiments performed on HCT116/E6 and HCT116 p21^{-/-} cells clearly indicate that p53 and p21^{CIP1/WAF1} are necessary for both Curcumin and DAC post-mitotic G1 arrest and for the direct G1/S block activated by bDMC (Fig. 6). We believe that a concurrent p53-dependent and -independent p21 transactivation occurs following Curcuminoids treatment. As in HCT116 p21^{-/-} compared to HCT116/E6 cells, only bDMC shows an increase of the replicative events, it is possible that a p53-independent activation of p21^{CIP1/WAF1} is required to maintain active the primary G1/S checkpoint. Conversely, the G1 post-mitotic arrest triggered *via* mitotic slippage by Curcumin, DAC and, to a lesser extent, by bDMC, induces the p21^{CIP1/WAF1} gene through the transcription factor p53 (Graphical abstract). This hypothesis is supported by ChIP analysis shown in Figure 6D: Curcumin and DAC exposure induces the binding of p53 on the p21^{CIP1/WAF1} promoter, whereas upon bDMC treatment only a faint recruitment is observed.

Western blot and immunofluorescence assays detect the activation of a DNA damage response elicited upon mitotic impairment for Curcumin and DAC (Figure 5). It is tempting to speculate that DNA damage is activated as an effect of a severe mitotic block induced by Curcumin and DAC, but it is not clear if DNA damage occurs in mitotic or post-mitotic G1 arrested cells. Compared with the DNA damage responses during G1 and G2, considerably less is known about the DNA damage activation during mitosis. As bDMC is concerned, DNA damage is observed concurrently to the cell cycle impairment, thus pointing this molecule as a both spindle-disrupting and DNA-damaging drug. There is strong evidence highlighting that DNA damage occurred in mitotic cells inhibits mitotic exit after the block is removed and that this delay is not an ATM-dependent mechanism [50, 51]. This is coherent with our data showing that bDMC induces a long-lasting G2/M block, which is not reverted by caffeine pretreatment. We can't rule out that DNA damage is triggered in G1 arrested cells (Graphical abstract). This hypothesis need further investigation to elucidate the events and regulatory mechanisms of bDMC effects on cell cycle progression, which ensure its possible development in anti-cancer clinical applications.

Acknowledgments

This work was supported by AIRC-MFAG (My First AIRC Grant). Special thanks to Prof. R. Mantovani (University of Milan) and Prof. Monica Saladini (University of Modena and Reggio Emilia) for scientific suggestions and helpful discussion. We are thankful to “Centro Interdipartimentale Grandi Strumenti (CIGS)” of the University of Modena and Reggio Emilia and to the “Fondazione Cassa di Risparmi di Modena” which supplied NMR Spectrometer.

Accepted Manuscript

References

- [1] Jordan MA, Wilson L. Microtubules as a target for anticancer drugs. *Nat Rev Cancer* 2004;4:253-65.
- [2] Gupta KK, Bharné SS, Rathinasamy K, Naik NR, Panda D. Dietary antioxidant curcumin inhibits microtubule assembly through tubulin binding. *FEBS J* 2006;273:5320-32.
- [3] Holy JM. Curcumin disrupts mitotic spindle structure and induces micronucleation in MCF-7 breast cancer cells. *Mutat Res* 2002;518:71-84.
- [4] Hanif R, Qiao L, Shiff SJ, Rigas B. Curcumin, a natural plant phenolic food additive, inhibits cell proliferation and induces cell cycle changes in colon adenocarcinoma cell lines by a prostaglandin-independent pathway. *J Lab Clin Med* 1997;130:576-84.
- [5] Cheng AL, Hsu CH, Lin JK, Hsu MM, Ho YF, Shen TS, et al. Phase I clinical trial of curcumin, a chemopreventive agent, in patients with high-risk or pre-malignant lesions. *Anticancer Res* 2001;21:2895-900.
- [6] Sharma RA, Euden SA, Platton SL, Cooke DN, Shafayat A, Hewitt HR, et al. Phase I clinical trial of oral curcumin: biomarkers of systemic activity and compliance. *Clin Cancer Res* 2004;10:6847-54.
- [7] Sahu RP, Batra S, Srivastava SK. Activation of ATM/Chk1 by curcumin causes cell cycle arrest and apoptosis in human pancreatic cancer cells. *Br J Cancer* 2009;100:1425-33.
- [8] Aggarwal BB, Kumar A, Bharti AC. Anticancer potential of curcumin: preclinical and clinical studies. *Anticancer Res* 2003;23:363-98.
- [9] Jee SH, Shen SC, Tseng CR, Chiu HC, Kuo ML. Curcumin induces a p53-dependent apoptosis in human basal cell carcinoma cells. *J Invest Dermatol* 1998;111:656-61.
- [10] Kawamori T, Lubet R, Steele VE, Kelloff GJ, Kaskey RB, Rao CV, et al. Chemopreventive effect of curcumin, a naturally occurring anti-inflammatory agent, during the promotion/progression stages of colon cancer. *Cancer Res* 1999;59:597-601.

- [11] Mehta K, Pantazis P, McQueen T, Aggarwal BB. Antiproliferative effect of curcumin (diferuloylmethane) against human breast tumor cell lines. *Anticancer Drugs* 1997;8:470-81.
- [12] Singletary K, MacDonald C, Iovinelli M, Fisher C, Wallig M. Effect of the beta-diketones diferuloylmethane (curcumin) and dibenzoylmethane on rat mammary DNA adducts and tumors induced by 7,12-dimethylbenz[a]anthracene. *Carcinogenesis* 1998;19:1039-43.
- [13] Hayun R, Okun E, Berrebi A, Shvidel L, Bassous L, Sredni B, et al. Rapamycin and curcumin induce apoptosis in primary resting B chronic lymphocytic leukemia cells. *Leuk Lymphoma* 2009;50:625-32.
- [14] Purkayastha S, Berliner A, Fernando SS, Ranasinghe B, Ray I, Tariq H, et al. Curcumin Blocks Brain Tumor Formation. *Brain Res* 2009.
- [15] Li ZX, Ouyang KQ, Jiang X, Wang D, Hu Y. Curcumin induces apoptosis and inhibits growth of human Burkitt's lymphoma in xenograft mouse model. *Mol Cells* 2009;27:283-9.
- [16] Lin YT, Wang LF, Hsu YC. Curcuminoids Suppress the Growth of Pharynx and Nasopharyngeal Carcinoma Cells through Induced Apoptosis. *J Agric Food Chem* 2009.
- [17] Mann CD, Neal CP, Garcea G, Manson MM, Dennison AR, Berry DP. Phytochemicals as potential chemopreventive and chemotherapeutic agents in hepatocarcinogenesis. *Eur J Cancer Prev* 2009;18:13-25.
- [18] Srivastava RK, Chen Q, Siddiqui I, Sarva K, Shankar S. Linkage of curcumin-induced cell cycle arrest and apoptosis by cyclin-dependent kinase inhibitor p21(WAF1/CIP1). *Cell Cycle* 2007;6:2953-61.
- [19] Shishodia S, Amin HM, Lai R, Aggarwal BB. Curcumin (diferuloylmethane) inhibits constitutive NF-kappaB activation, induces G1/S arrest, suppresses proliferation, and induces apoptosis in mantle cell lymphoma. *Biochem Pharmacol* 2005;70:700-13.
- [20] Sa G, Das T. Anti cancer effects of curcumin: cycle of life and death. *Cell Div* 2008;3:14.
- [21] Sharma RA, Gescher AJ, Steward WP. Curcumin: the story so far. *Eur J Cancer* 2005;41:1955-68.

- [22] Shishodia S, Sethi G, Aggarwal BB. Curcumin: getting back to the roots. *Ann N Y Acad Sci* 2005;1056:206-17.
- [23] Wang YJ, Pan MH, Cheng AL, Lin LI, Ho YS, Hsieh CY, et al. Stability of curcumin in buffer solutions and characterization of its degradation products. *J Pharm Biomed Anal* 1997;15:1867-76.
- [24] Blasius R, Duvoix A, Morceau F, Schnekenburger M, Delhalle S, Henry E, et al. Curcumin stability and its effect on glutathione S-transferase P1-1 mRNA expression in K562 cells. *Ann N Y Acad Sci* 2004;1030:442-8.
- [25] Anand P, Thomas SG, Kunnumakkara AB, Sundaram C, Harikumar KB, Sung B, et al. Biological activities of curcumin and its analogues (Congeners) made by man and Mother Nature. *Biochem Pharmacol* 2008;76:1590-611.
- [26] Yodkeeree S, Chaiwangyen W, Garbisa S, Limtrakul P. Curcumin, demethoxycurcumin and bisdemethoxycurcumin differentially inhibit cancer cell invasion through the down-regulation of MMPs and uPA. *J Nutr Biochem* 2009;20:87-95.
- [27] Mishra S, Narain U, Mishra R, Misra K. Design, development and synthesis of mixed bioconjugates of piperic acid-glycine, curcumin-glycine/alanine and curcumin-glycine-piperic acid and their antibacterial and antifungal properties. *Bioorg Med Chem* 2005;13:1477-86.
- [28] Sumanont Y, Murakami Y, Tohda M, Vajragupta O, Matsumoto K, Watanabe H. Evaluation of the nitric oxide radical scavenging activity of manganese complexes of curcumin and its derivative. *Biol Pharm Bull* 2004;27:170-3.
- [29] Vajragupta O, Boonchoong P, Berliner LJ. Manganese complexes of curcumin analogues: evaluation of hydroxyl radical scavenging ability, superoxide dismutase activity and stability towards hydrolysis. *Free Radic Res* 2004;38:303-14.
- [30] Mishra S, Kapoor N, Mubarak Ali A, Pardhasaradhi BV, Kumari AL, Khar A, et al. Differential apoptotic and redox regulatory activities of curcumin and its derivatives. *Free Radic Biol Med* 2005;38:1353-60.

- [31] Basile V, Mantovani R, Imbriano C. DNA damage promotes histone deacetylase 4 nuclear localization and repression of G2/M promoters, via p53 C-terminal lysines. *J Biol Chem* 2006;281:2347-57.
- [32] Benatti P, Basile V, Merico D, Fantoni LI, Tagliafico E, Imbriano C. A balance between NF- κ B and p53 governs the pro- and anti-apoptotic transcriptional response. *Nucleic Acids Res* 2008;36:1415-28.
- [33] Hsu YC, Weng HC, Lin S, Chien YW. Curcuminoids-cellular uptake by human primary colon cancer cells as quantitated by a sensitive HPLC assay and its relation with the inhibition of proliferation and apoptosis. *J Agric Food Chem* 2007;55:8213-22.
- [34] Kunwar A, Barik A, Mishra B, Rathinasamy K, Pandey R, Priyadarsini KI. Quantitative cellular uptake, localization and cytotoxicity of curcumin in normal and tumor cells. *Biochim Biophys Acta* 2008;1780:673-9.
- [35] Weaver BA, Cleveland DW. Decoding the links between mitosis, cancer, and chemotherapy: The mitotic checkpoint, adaptation, and cell death. *Cancer Cell* 2005;8:7-12.
- [36] Brito DA, Rieder CL. Mitotic checkpoint slippage in humans occurs via cyclin B destruction in the presence of an active checkpoint. *Curr Biol* 2006;16:1194-200.
- [37] Andreassen PR, Lacroix FB, Lohez OD, Margolis RL. Neither p21WAF1 nor 14-3-3sigma prevents G2 progression to mitotic catastrophe in human colon carcinoma cells after DNA damage, but p21WAF1 induces stable G1 arrest in resulting tetraploid cells. *Cancer Res* 2001;61:7660-8.
- [38] Vogel C, Kienitz A, Hofmann I, Muller R, Bastians H. Crosstalk of the mitotic spindle assembly checkpoint with p53 to prevent polyploidy. *Oncogene* 2004;23:6845-53.
- [39] Meek DW. The role of p53 in the response to mitotic spindle damage. *Pathol Biol (Paris)* 2000;48:246-54.
- [40] Dalton WB, Nandan MO, Moore RT, Yang VW. Human cancer cells commonly acquire DNA damage during mitotic arrest. *Cancer Res* 2007;67:11487-92.

- [41] Rieder CL, Maiato H. Stuck in division or passing through: what happens when cells cannot satisfy the spindle assembly checkpoint. *Dev Cell* 2004;7:637-51.
- [42] Shiloh Y. The ATM-mediated DNA-damage response: taking shape. *Trends Biochem Sci* 2006;31:402-10.
- [43] Zhou BB, Elledge SJ. The DNA damage response: putting checkpoints in perspective. *Nature* 2000;408:433-9.
- [44] Ahn J, Urist M, Prives C. The Chk2 protein kinase. *DNA Repair (Amst)* 2004;3:1039-47.
- [45] Watson JL, Hill R, Lee PW, Giacomantonio CA, Hoskin DW. Curcumin induces apoptosis in HCT-116 human colon cancer cells in a p21-independent manner. *Exp Mol Pathol* 2008;84:230-3.
- [46] Sharma RA, McLelland HR, Hill KA, Ireson CR, Euden SA, Manson MM, et al. Pharmacodynamic and pharmacokinetic study of oral Curcuma extract in patients with colorectal cancer. *Clin Cancer Res* 2001;7:1894-900.
- [47] Sharma RA, Steward WP, Gescher AJ. Pharmacokinetics and pharmacodynamics of curcumin. *Adv Exp Med Biol* 2007;595:453-70.
- [48] Ireson C, Orr S, Jones DJ, Verschöyle R, Lim CK, Luo JL, et al. Characterization of metabolites of the chemopreventive agent curcumin in human and rat hepatocytes and in the rat in vivo, and evaluation of their ability to inhibit phorbol ester-induced prostaglandin E2 production. *Cancer Res* 2001;61:1058-64.
- [49] Liang G, Shao L, Wang Y, Zhao C, Chu Y, Xiao J, et al. Exploration and synthesis of curcumin analogues with improved structural stability both in vitro and in vivo as cytotoxic agents. *Bioorg Med Chem* 2009;17:2623-31.
- [50] Mikhailov A, Cole RW, Rieder CL. DNA damage during mitosis in human cells delays the metaphase/anaphase transition via the spindle-assembly checkpoint. *Curr Biol* 2002;12:1797-806.
- [51] Smits VA, Klompmaker R, Arnaud L, Rijksen G, Nigg EA, Medema RH. Polo-like kinase-1 is a target of the DNA damage checkpoint. *Nat Cell Biol* 2000;2:672-6.

Figure legends

Fig. 1. Structures of Curcumin, bDMC and DAC.

Fig. 2. UV-vis spectroscopic study on stability and uptake of Curcuminoids in HCT116 cells. **(A)** Left panel. UV-vis absorption spectra of Curcumin extracted from control medium at time zero (a), 4 hours (b) and 24 hours (c) and (right panel) linear relationships between the absorbance values (420 nm) and concentration at time zero (●), 4 hours (○) and 24 hours (▼). **(B)** Confocal microscopy analysis of Curcumin, bDMC and DAC cellular uptake. **(C)** Percentages of Curcumin, bDMC and DAC extracted from culture medium and HCT116 cells at 20 μ M and 30 μ M concentrations; all data are the mean of three independent experiments and are normalized to the control. **(D)** Curcuminoids extracted from HCT116 cells at different time courses and concentrations; percentages are referred to time zero extracts for each drug.

Fig. 3. Biological effects of Curcumin (10 μ M), bDMC (30 μ M) and DAC (10 μ M) in HCT116 cells. **(A)** Microscopic analysis of the nuclear morphology and microtubule spindles formation of HOECHST/ α -tubulin stained cells after drugs incubation (magnification 100X). Bar, 15.80 μ m. Monopolar spindles are indicated by the arrows. **(B)** Flow cytometric analysis of cell cycle progression following Curcumin, bDMC and DAC treatments for 24 hours. Data represent means \pm SD of ten independent experiments. **(C)** DNA distribution analysis of PI/BrdU stained cells after 24 hours drugs exposure. **(D)** Western blot analysis of Phospho-Ser10 H3 and H2A expression levels upon drugs incubation. The value under each band indicates the relative expression level of Phospho-Ser10 H3 normalized by the intensity of H2A in each lane. The normalized intensity in the first lane was set as relative expression level of 1.

Fig. 4. bDMC induces a concomitant G2/M and G1/S arrest. **(A)** Distribution of BrdU positive and negative cells in G1 phase after drugs treatment. Results are mean \pm SD of three independent experiments. **(B)** Western blot and RT-PCR analysis of Cyclin B1 expression after drugs treatment. The intensity of immunoreactive and RT-PCR bands have been quantitated to actin and GAPDH respectively. The normalized intensity in the first lane was set as relative expression level of 1. Values, mean of four independent experiments, * $P < 0.05$, ** $P < 0.01$ vs DMSO. **(C)** Distribution of

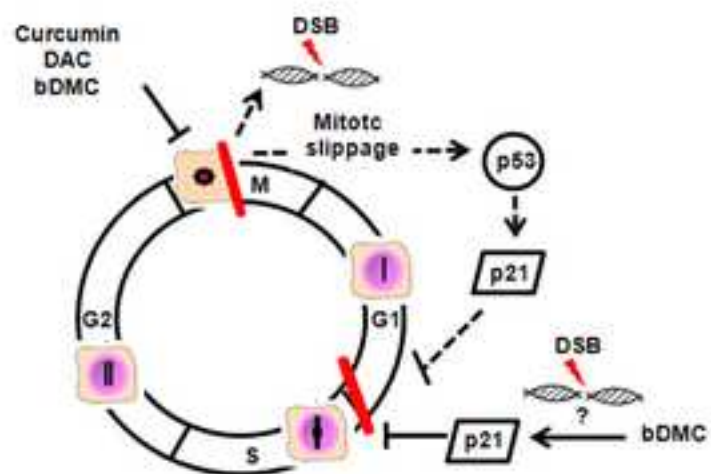
cells in G0/G1 (left panel) and G2/M (right panel) phases after the release (4-8-10-12 hours) from 24 hours drugs exposure. **(D)** DNA distribution analysis of PI/BrdU stained cells after G0/G1 synchronization and release in drugs-added media.

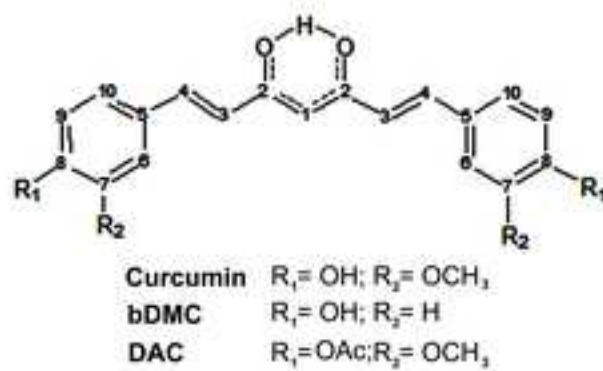
Fig. 5. bDMC induces rapid DNA double-strand breaks. **(A)** γ -H2AX and total H2A protein expression analysis of acid extracts following 24 hours drugs exposure. **(B)** Left panel: immunofluorescence analysis of γ -H2AX and HOECHST staining after 8, 16 and 24 hours treatments with Curcumin, bDMC and DAC (magnification 40X). Bar, 100 μ m. Right panel: cell cycle distribution of PI stained cells after the indicated time-course drugs incubation. **(C)** Western blot analysis of control and treated HCT116 total extracts with anti-phospho-ATM, anti-p53 and anti-actin antibodies. **(D)** Distribution of cells in G2/M phase after Curcuminoids and caffeine/Curcuminoids co-treatment for 24 hours.

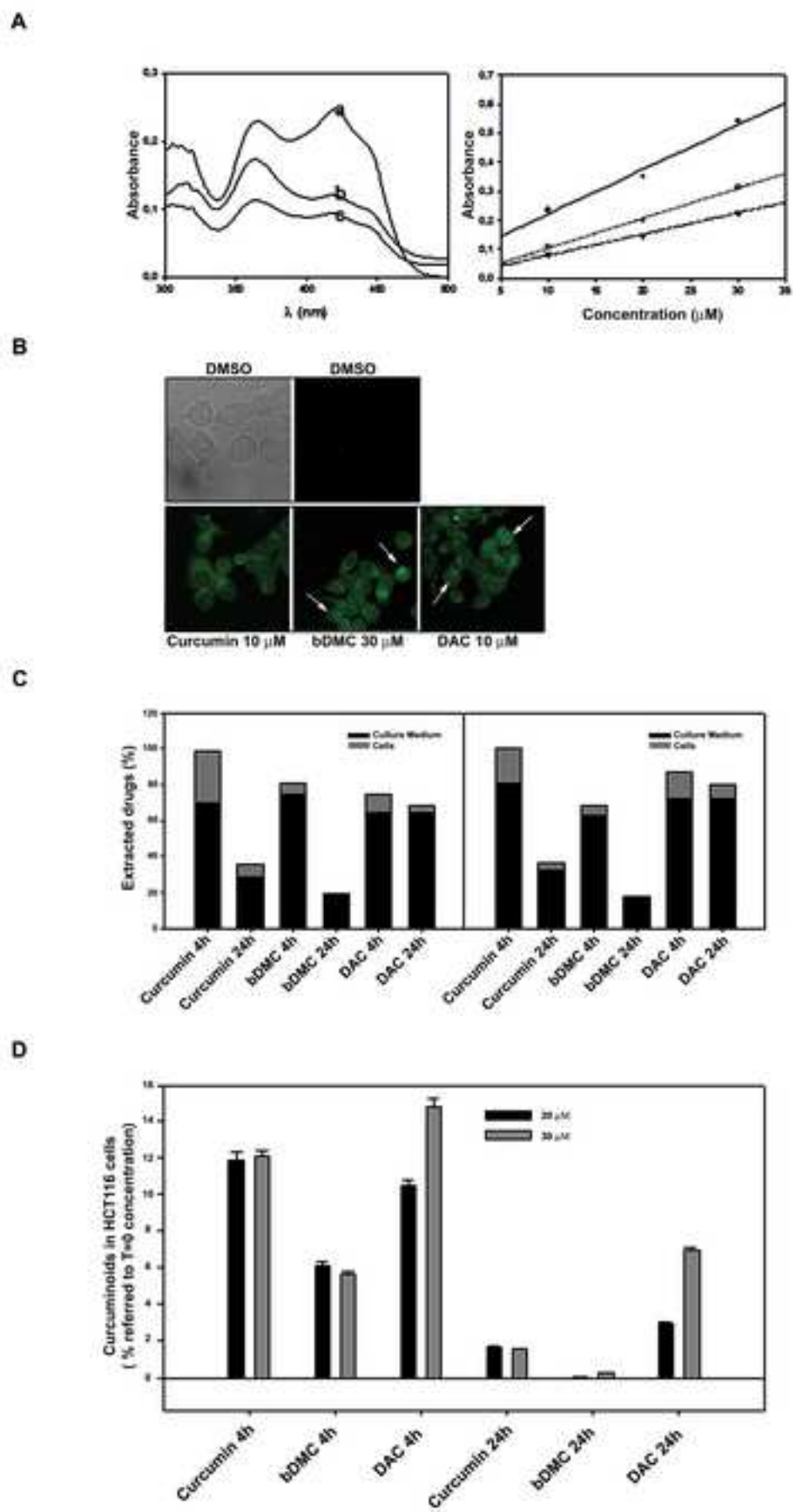
Fig. 6. Role of p53 and p21^{CIP1/WAF1} in the anti-proliferative effects of Curcumin and its derivatives. **(A)** Flow cytometric analysis of HCT116/E6 cell cycle progression following Curcumin, bDMC, DAC and nocodazole treatments. Data represent means \pm SD of three independent experiments. **(B)** p21 expression analysis of protein and mRNA levels of HCT116 and HCT116/E6 by western blot (left panel) and RT-PCR (right panel). The actin protein and GAPDH mRNA were used as internal controls. **(C)** Cell cycle distribution of PI stained HCT116 p21^{-/-} cells after 24 hours drugs exposure. **(D)** ChIP analysis of p53 binding to p21^{CIP1/WAF1} promoter after DMSO, Curcumin, bDMC and DAC exposure.

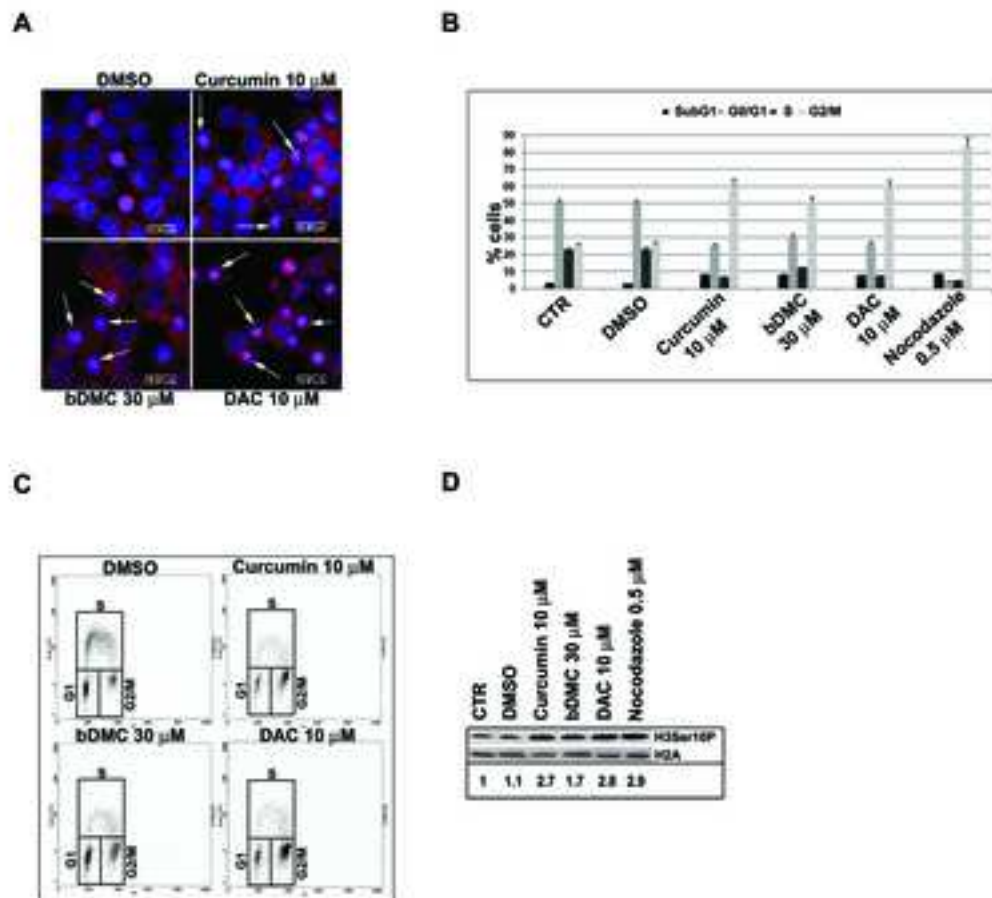
Graphical abstract. Model of the molecular mechanism through which Curcumin, DAC and bDMC induce cell cycle arrest in human colon cancer cells. Bold lines indicate the direct effects of the molecules, dotted lines represent the consequences of the induced mitotic delay.

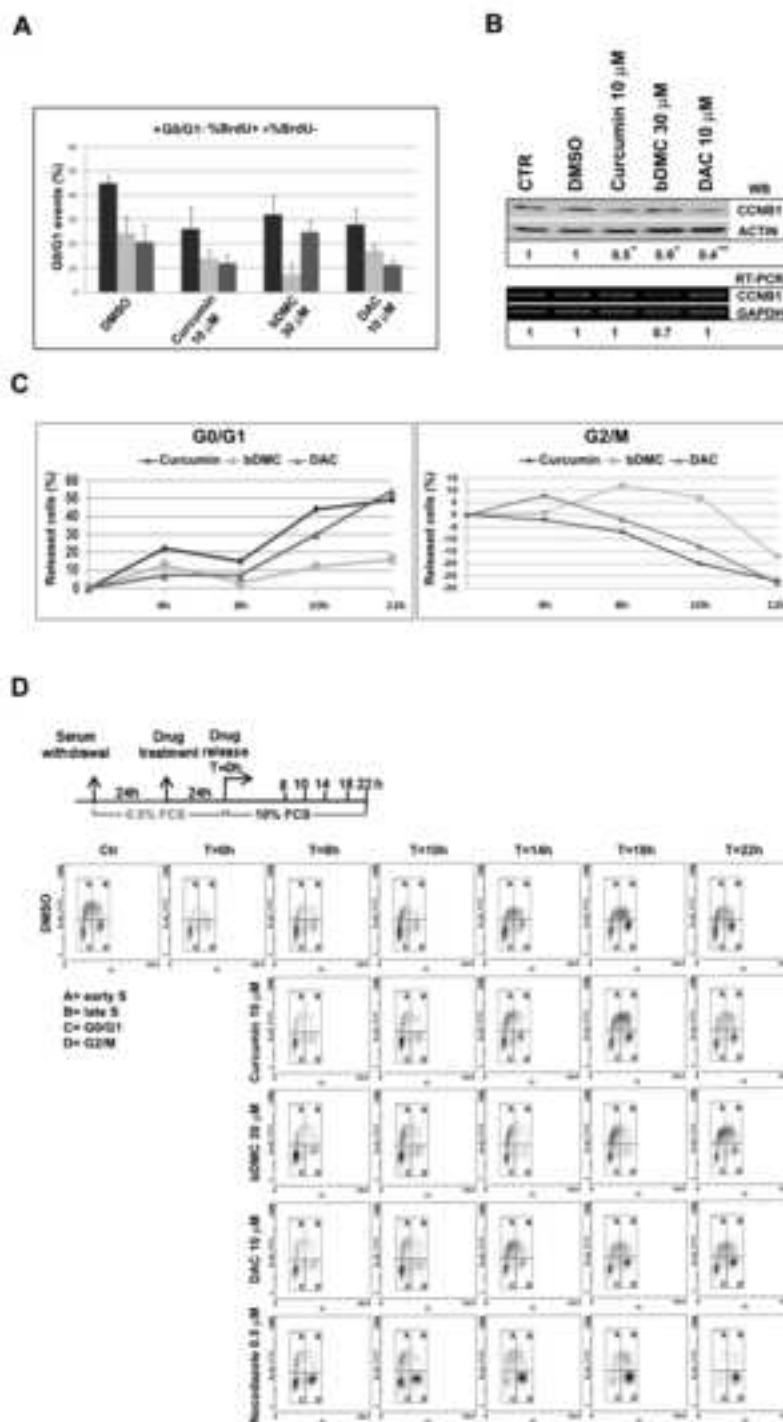
Supplementary Fig.1. Curcuminoids dose-response flow cytometric analysis. Cell cycle distribution analysis upon dose-response treatments for 24 hours with DMSO, Curcumin (5-10-20 μ M), bDMC (20-30-40 μ M) and DAC (5-10-20 μ M). Data represent means \pm SD of three independent experiments.

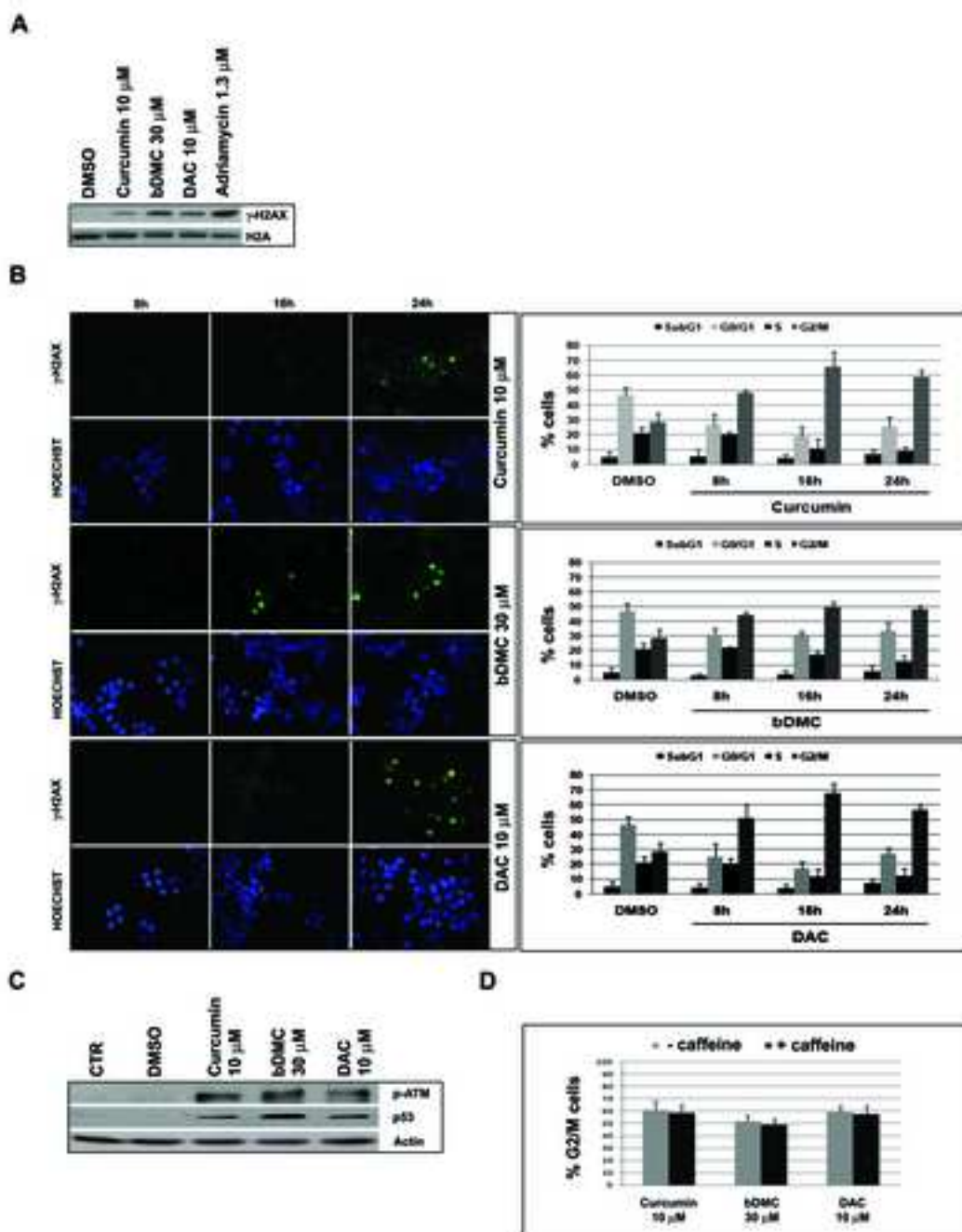




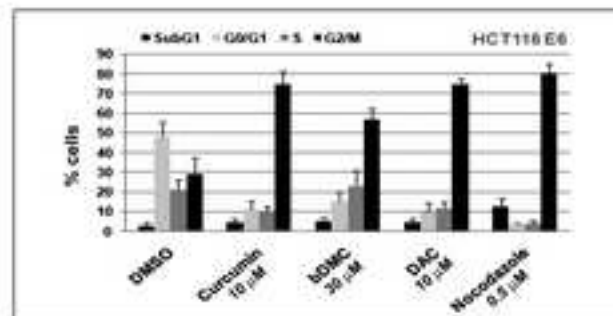




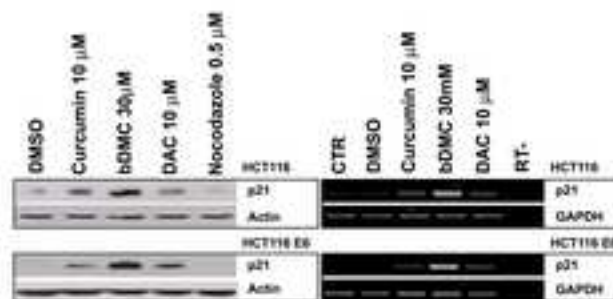




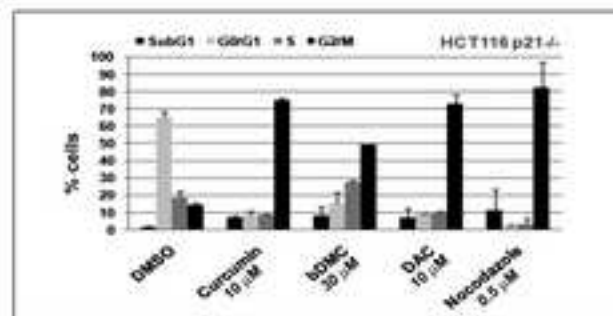
A



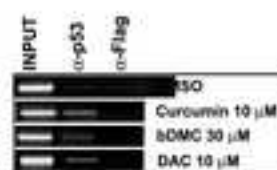
B



C



D



A

